Capillary Forces Between Two Solid Spheres Linked by a Concave Liquid Bridge: Regions of Existence and Forces Mapping

David Megias-Alguacil and Ludwig J. Gauckler
Non-Metallic Inorganic Materials, Dept. of Materials, ETH-Zürich, Zürich 8093, Switzerland

DOI 10.1002/aic.11726
Published online March 23, 2009 in Wiley InterScience (www.interscience.wiley.com).

This article focuses on the capillary interactions arising when two spherical particles are connected by a concave liquid bridge. This scenario is found in many situations where particles are partially wetted by a liquid, like liquid films stabilized with nanoparticles. We analyze different parameters governing the liquid bridge: interparticle separation, wetting angle and liquid volume. The results are compiled in a liquid volume-wetting angle diagram in which the regions of existence (stability) or inexistence (instability) of the bridge are outlined and the possible maximum and minimal particle distances for which the liquid bridge may be found. Calculations of the capillary forces discriminate those conditions for which such force is repulsive or attractive. The results are plotted in form of maps that allow an easy understanding of the stability of a liquid bridge and the conditions at which it may be produced for the two particle model. © 2009 American Institute of Chemical Engineers *AIChE J,* 55: 1103–1109, 2009
Keywords: liquid bridge, capillary force, wetting force, Laplace, nanoparticle, mapping

Introduction

The insertion of fine particles in between a liquid film modifies the film geometry, which further forms a liquid bridge with a curved meniscus shape. The contact between the three phases, solid, liquid, and gas, induces the onset of forces between these particles, which will depend on physical-chemical aspects like the wettability of the particles, the geometry of the meniscus as well as the particles size and separation between them.

This scenario has gained an increased attention in the past years because it may be found in many practical situations, which reveals itself as very important to understand the behavior of a wide variety of systems, like e.g. liquid phase sintering,[1] liquid foams and emulsions,[2] and many others.

Capillary forces between pairs of particles due to a liquid bridge have been investigated by different authors, i.e.[1,3–14] The aim of the present work is to contribute to this topic by going beyond the mere calculus of such capillary forces, exploring the conditions for which a concave liquid bridge may exist or not. For such a task, we will provide an original expression for the minimum interparticle distance, not yet reported in literature to our best knowledge, which together with an existing expression for the maximum distance reachable by the particles joined by the bridge, will allow us to build those regions of possible existence of the bridge, in terms of novel relative liquid volume and wetting angle diagrams. Afterwards, once identified the corresponding existence regions, the interparticle capillary force will be calculated where appropriate, and according to these results, we will build new liquid volume-wetting angles maps where displaying those regions of attraction/repulsion force character.

Description of the System and Calculus of Meniscus Geometries

We consider a linear string of aligned solid monosized round particles. The particles are partially wetted by the

Correspondence concerning this article should be addressed to D. Megias-Alguacil david.megias@mat.ethz.ch

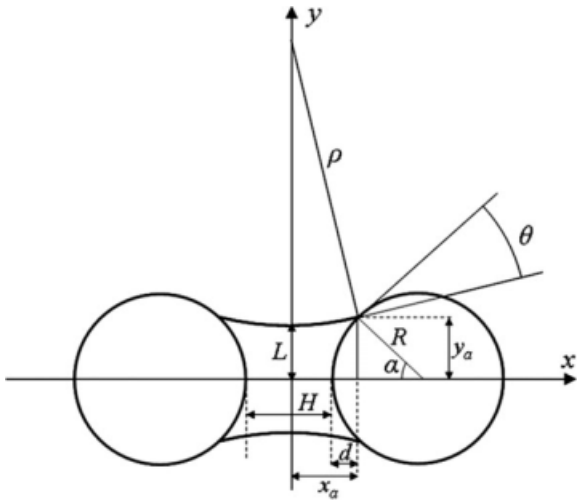

Figure 1. Sketch of the liquid bridge geometry, where displayed the parameters involved in the calculations.

liquid, which forms a liquid bridge between the spheres in the so-called pendular state (where the liquid phase is discontinuous). This is the scenario which may be found in a bubble covered with small solid particles, provided the size of the bubble much bigger than the particle size. Considering that the particles are very small, the effect of gravity is negligible, and no other buoyancy force will be considered. In such a case, the liquid bridge has a constant pressure[15] and the meniscus posses the shape of a surface of revolution[16,17] with the same mean curvature everywhere.[10] The meniscus shape is defined as an arc of one o the Delaunay's surfaces,[18] which are generated by the rotation around the basis of the Delaunay's roulettes.[15] Also, other axisymmetric profiles of uniform mean curvature, like the nodoid, catenoid, or unduloid, have been considered.[10] In the present work, for sake of simplicity, we will assume a meniscus profile described by an arc of circumference, as sketched in Figure 1, under the assumption that the error brought about by this approximation is small in most cases.[1,10,16,19]

We will consider air as the gaseous phase and that the stable liquid bridge features a concave shaped meniscus with wetting angles smaller than 90°, since hydrophobic solid particles behaves as antifoamers.[20]

As displayed in Figure 1, R is the solid particle's radius, x_a and y_a are the abscissa and coordinate of the contact point between the solid and liquid profile, respectively, α is the half-filling angle, θ is the wetting angle, ρ and L are the principal radius of the liquid meniscus, measured orthogonally. H is the surface-to-surface distance between the solid particles, and d is the wetted portion of each hemisphere. The reference system is chosen such its origin is the middle point between the spheres and whose x-axis lies along the straight line which joins the particles' centers, as shown in Figure 1.

Considering, for sake of simplicity, just the upper right quadrant, the liquid and solid profiles are described by the following equations:

$$y_{\mathrm{L}}(x) = (\rho + L) - \sqrt{\rho^2 - x^2} \tag{1}$$

for the liquid meniscus, and:

$$y_{\mathrm{S}}(x) = \sqrt{R^2 - \left(x - \frac{H}{2} - R\right)^2} \tag{2}$$

for the solid profile.

The principal radii, ρ and L, may be described in terms of both representative angles, α and θ, or on the other hand, by means of x_a. Indeed, geometrical considerations follow in the next relationships. The half-filling angle:

$$\alpha = \arccos\left(\frac{H/2 + R - x_a}{R}\right) \tag{3}$$

The radii are

$$\rho = \frac{x_a R}{(H/2 + R - x_a)\cos\theta - \sqrt{R^2 - (x_a - H/2 - R)^2}\sin\theta} \tag{4}$$

and

$$L = \sqrt{R^2 - (x_a - H/2 - R)^2} + x_a \frac{\sqrt{R^2 - (x_a - H/2 - R)^2}\cos\theta + (H/2 + R - x_a)\sin\theta - R}{(H/2 + R - x_a)\cos\theta - \sqrt{R^2 - (x_a - H/2 - R)^2}\sin\theta} \tag{5}$$

Let us point out here that the principal radius ρ is related to the concave–convex character of the liquid meniscus, meanwhile the radius L gives an indication of the meniscus thickness.

The liquid volume of the bridge, V, may be determined for a given distance between particles, H, by definite integration of both the solid and liquid profiles:

$$V = 2\pi \int_0^{x_a} [y_L(x)]^2 dx - 2\pi \int_{H/2}^{x_a} [y_S(x)]^2 dx \tag{6}$$

Introducing Eqs. 1–2 into Eq. 6, solving the integrals gives:

$$\frac{V}{2\pi} = \left[(\rho + L)^2 + \rho^2\right] x_a - \frac{x_a^3}{3} - (\rho + L)\left[x_a\sqrt{\rho^2 - x_a^2} + \rho^2 \arcsin\frac{x_a}{\rho}\right] - \frac{(x_a - H/2)^2}{3}[3R - (x_a - H/2)] \tag{7}$$

Substituting ρ and L by Eqs. 4 and 5, respectively, the volume of the liquid bridge is therefore expressed just as a function of the parameter x_a and the wetting angle, θ, at each interparticle separation H between the two equal spheres of radius R.

Different authors have calculated the liquid bridge volume, most of them in terms of the half-filling angle, α. Particularly, Pietsch and Rumpf[6] gave an expression for V in terms of α, which is fully equivalent to our Eq. 7, considering the relationship between x_a and α given by Eq. 3. Other authors have obtained simpler expressions than Eq. 7 making assumptions to simplify the calculation and being able of obtaining an explicit expression of V as a function of x_a, but unfortunately, they result in underestimated values[5] or overestimated ones,[21–23] respect to those obtained with the Eq. 7.

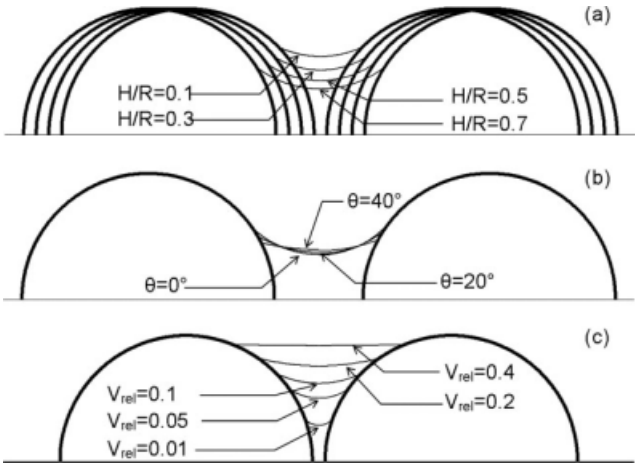

Figure 2. Meniscus and spheres profiles drawn at different conditions: (a) $\theta = 20^\circ$, $V_{rel} = 0.1$; (b) $V_{rel} = 0.1$, $H/R = 0.7$; (c) $\theta = 20^\circ$, $H/R = 0.1$.

It is not possible to derive an explicit expression for x_a from Eq. 7, for a given value of the liquid volume at a certain separation H and wetting angle θ. Thus, x_a must be calculated numerically. Once this value is obtained, the values of the other geometrical parameters, ρ and L, arise immediately by means of Eqs. 4 and 5.

On what it follows, we will refer to the liquid volume of the bridge throughout the relative volume, V_{rel}, of the liquid respect to the volume of the sphere, then, $V_{rel}=3V/(4\pi R^3)$.

Figure 2 displays some liquid bridges profiles for different situations, just considering the upper portion of the spheres and bridges, for sake of clarity. Observe from Figure 2a, that increasing the distance between the particles, for a given liquid volume and wetting angle, the meniscus reduces its radius L, as expected; the other principal radius, ρ, decreases for short distances H, for later increase as the separation between the particles gets larger, then showing a minimum at larger H for increasing liquid volumes. The overall effect of separating the particles while keeping constant the liquid volume is therefore an elongation of the bridge, which becomes longer and thinner and less concave.

The modification of the wetting angle, Figure 2b, supposed that both liquid volume and separation are fixed, is followed mainly by a strong decreasing of the meniscus curvature, being flattened as the wetting angle, θ, increases. As in the previous case, the contact point between the liquid and the solid reduces its coordinate x_a and y_a, as well as the half-filling angle, α, diminishes.

Finally, the effect of the liquid volume is shown in Figure 2c, where the interparticle distance and the wetting angle have been fixed. As expected, the increasing of the amount of liquid follows in increasing thicker meniscus (larger L) as well as an evident reduction of the meniscus curvature (larger ρ). If the amount of liquid is increased sufficiently, it may cover completely the spheres, and beyond this point, the spheres will be fully immersed in the liquid; this situation clearly does not correspond to a liquid bridge anymore. In other words, the bridge may no longer exist under this circumstance.

According to this discussion, it may be claimed that the liquid bridge has limits, that is, the existence of a liquid bridge for a certain value of liquid volume and wetting angle does not imply that this bridge may be found for all possible distances between the particles. These limits will be outlined in the next sections.

Regions of existence of a concave liquid bridge

When plotting the liquid volume calculated by means of Eq. 7 as a function i.e., of the half-filling angle, α, Figure 3 (for the cases $\theta = 20^\circ$ and $\theta = 40^\circ$ at several dimensionless distances H/R), it is observed that the liquid volume increases for all the interparticle distances as α enlarges, as expected. This trend stops at a certain value of the half-filling angle, i.e., at $\alpha = 70^\circ$ when $\theta = 20^\circ$, and $\alpha = 50^\circ$ when $\theta = 40^\circ$, indicating the limiting filling of the space between both solid particles. Indeed, it is clear that the concave liquid bridge cannot hold any amount of liquid for a certain wetting angle and separation between the particles. Another situation arises in case of an excess of liquid should be followed by an overfilling of the gap between particles, and the system should tend to transform into a typical bulk suspension. Even another possibility is that the shape of the liquid meniscus changes towards a convex profile, a situation which we will not be allowed in our further considerations.

To delimitate the maximum amount of liquid, V_{max}, which may be hold by a bridge compatible with the preservation of the wetting angle, we consider a limit half-filling angle, α_{limit}, that can be simply obtained by imposing the critical condition $\rho \to \infty$. This corresponds to a liquid bridge with a cylindrical shape, border case between the concave and convex meniscus. Geometrically, Figure 1, it is straight forward to obtain that the limit half-filling angle is:

$$\alpha_{limit} = \frac{\pi}{2} - \theta \tag{8}$$

For the particular case $\theta = 20^\circ$, $\alpha_{limit} = 70^\circ$, which agrees with the finding in Figure 3.

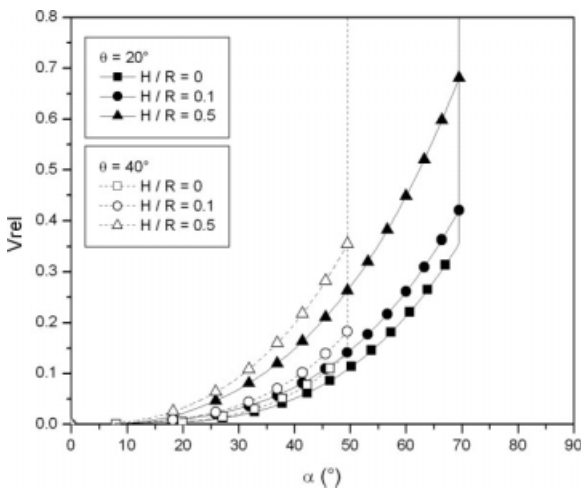

Figure 3. Relative liquid volume, V_{rel}, as a function of the half-filling angle, α, for several dimensionless interparticle distances and two wetting angles, $\theta = 20^\circ$ and $\theta = 40^\circ$.

The maximum liquid volume, V_{max}, can then be determined considering such a cylindrical bridge of radius y_a and length $H + 2d$, ended with two spherical caps of height d. Thus, taking into account the corresponding volumes of these geometrical bodies, we have:

$$V_{max} = 2\pi\, x_a\, y_a^2 - \frac{2}{3}\pi\, d^2\, (3R - d) \tag{9}$$

Considering that x_a, y_a, and d are (Figure 1):

$$\left.\begin{aligned} x_a &= \frac{H}{2} + R - R\cos\alpha \\ y_a &= R\sin\alpha \\ d &= R - R\cos\alpha \end{aligned}\right\} \tag{10}$$

and that α is in this case $\alpha_{limit} = \pi/2 - \theta$, Eq. 8, the maximum volume of liquid that the bridge may sustain at each surface-to-surface distance, H, and wetting angle, θ, is:

$$V_{max,rel} = \frac{1}{2}\left(3\cos^2\theta\,\left[\frac{H}{2R} + (1 - \sin\theta)\right] - (1 - \sin\theta)^2(2 + \sin\theta)\right) \tag{11}$$

where V_{max} has been made dimensionless by dividing by the sphere's volume. On view of Eq. 11, larger separations enable higher amounts of liquid, same trend than decreasing the wetting angle at a certain distance, H.

If considering the situation from the point of view of the distances instead of the volumes, one can realize that the separation H which appears in Eq. 11 corresponds to the minimum distance at which the particles can stay for a certain amount of liquid in a stable situation. Indeed, when a certain relative volume of liquid in respect to the solid volume and wetting angle are imposed, the particles must locate, at least, at distances $H \geq H_{min}$. Thus, we can re-write Eq. 11 to obtain an explicit expression for H_{min}:

$$\frac{H_{min}}{R} = 2\left[\frac{2V_{max,rel} + (1 - \sin\theta)^2(2 + \sin\theta)}{3\cos^2\theta} - (1 - \sin\theta)\right] \tag{12}$$

Notice from Figure 3 that larger distances between the particles are able to hold more liquid, in agreement with Eq. 12.

If by any reason, the particles are closer than this separation H_{min}, the particles should move apart from each other until the condition $H \geq H_{min}$ is satisfied, if the condition of having a concave meniscus is demanded. In case that the particles are not allowed to displace because i.e., spatial restrictions due to their number and/or distribution, there exists an excess of liquid which should induce a change of meniscus geometry, this becoming convex, or in case that the liquid amount is highly excessive, the system should evolve towards a suspension of solid particles fully immersed in the liquid and the liquid bridge configuration is destroyed.

Figure 4 displays a map diagram with some of those relative minimum distances, H_{min}/R, calculated using Eq. 12.

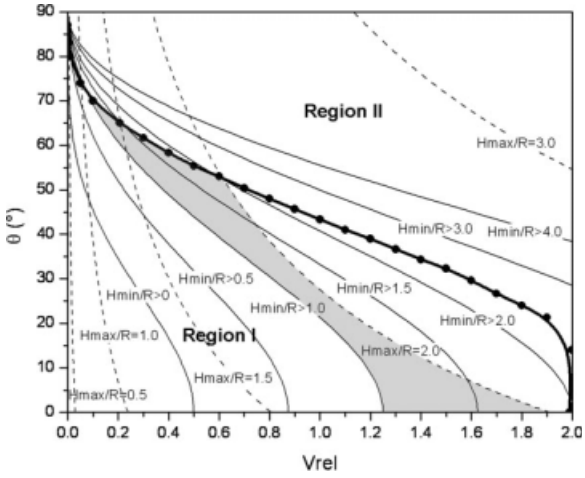

Figure 4. Map, $\theta - V_{rel}$, showing the combination of dimensionless minimum (solid lines), H_{min}/R, and maximum (dotted lines) distances, H_{max}/R, between which the liquid bridges may be found.

The solid symbol line represents the frontier between regions of existence (Region I) or inexistence (Region II) of the bridge. Shadowed area: see text.

There, the solid lines show the pairs $V_{rel} - \theta$ which delimit the values of liquid volume and wetting angle where a liquid bridge may be found at distances higher (restrictive condition) than those indicated by the corresponding line. As an example: a liquid bridge with $V_{rel} = 1.5$ and $\theta = 30°$ can only be found at distances larger than 2 times the particle radius R ($H/R > 2$). The values of the portion limited by the curve $H/R > 0$ and both axis correspond to the situation in which the bridge can be found when the particles are in contact.

In contrast, the bridge cannot be elongated indefinitely, and therefore, it exists a maximum distance between particles, beyond that the liquid bridge breaks, H_{break}. There have been efforts about the determination of this maximum distance, i.e., considering numerical evaluations of the solutions of the Young–Laplace equation[8] or the distance at which the half-filling angle, α, is a minimum.[12] The rupture of the liquid film occurs when the distance between the particles is large enough.[24] Lian et al.[25] proposed the following expression for moderate wetting angles:

$$\frac{H_{break}}{R} = \left(1 + \frac{\theta}{2}\right)\sqrt[3]{\frac{4}{3}\pi\, V_{rel}} \tag{13}$$

This Eq. 13 was found to agree with some experimental and theoretical work[17,26,27] based on the well-known Rayleigh instabilities suffered by a stretched cylindrical filament, and therefore it will be used in this work.

We draw the Eq. 13 in Figure 4 (dotted lines) , and observe that the distances at which the liquid bridges break increase when increasing the liquid volume, V_{rel}, and the wetting angle, θ. Assuming the Rayleigh instabilities as the main reason for the bridge rupture, it follows that the effect of such instabilities is more pronounced when the filament becomes thinner, which is the case of a liquid bridge of

small liquid volume and/or wetting angle, situations in which the meniscus thickness, identified with the radius L, gets smaller. We have also checked the behavior of the liquid bridge for unrestricted distances, and we found that there is a certain separation beyond that the liquid volume is not longer preserved, and the height of the contact point between the liquid and the solid surface, y_a, Figure 1, is zero. This distance is larger than H_{break}, Eq. 13, and shorter than the Rayleigh–Plateau limit ($H < 2\pi L$), this latter result was also found by Chen et al.[28]

With the combination of minimum and maximum distances, Figure 4 becomes a map which reflects what combinations of liquid amounts, V_{rel}, and wetting angles, θ, are able to produce a liquid bridge between certain interparticle distances, $H_{min}/R < H/R < H_{max}/R$. shown in Figure 4. the lines which delimit the minimum distances (solid lines) cross those lines which indicate the break or maximum distances (dashed lines). The line which connects the points where $H_{min} = H_{break}$ (symbols) is the frontier between two regions: one below such a border line, Region I, which corresponds to possible combinations of liquid volume, V_{rel}, and wetting angle, θ, which follow in a liquid bridge with a concave shape; and another region, Region II, where the bridge cannot preserve such a geometrical form. Also notice that a point belonging to Region II should need larger distances H_{min} than the bridge rupture distance, H_{break}, which obviously has not any meaning.

Figure 4 indicates that when the wetting angle is very high, only liquid bridges poor in liquid content can be formed. On contrary, a reduction of θ allows higher amounts of liquid. Interesting to note is the fact that a bridge with a liquid volume more than double that the sphere's volume is not possible to exist, for any wetting angle.

Figure 4 offers the regions of existence of liquid bridges. The shadowed area in Figure 4 is an exemplary case of the region of existence of liquid bridges: a liquid bridge whose liquid content and wetting angle belongs to such an area may exist only for distances larger than 1 particle radius and smaller than $2R$.

These results allow discriminating if for a certain pair $V_{rel} - \theta$, a concave liquid bridge may exist, and in such a positive case, between which ranges of interparticle distances the bridge may be found.

Forces mapping

Once the geometrical parameters which describe the liquid bridge (inside Region I) are calculated for a certain value of particle size and separation, wetting angle and relative volume of liquid respect to the solid sphere volume, the capillary forces between a pair of solid particles arising from the interaction between the solid and liquid surfaces may be calculated. On what it follows, negative forces indicate attraction whereas a positive force is repulsive.

It is well known, that the capillary force consists of two components. The first is a surface tension term acting at the wetting perimeter, tangent to the meniscus at the intersection with the solid surface and directed towards the liquid. The second component comes from the pressure difference across the curved air-liquid interface, which can be described by the Laplace–Young equation, computed over the axially projected wetted area of each particle. Thus, the total capillary force may be expressed in dimensionless form as:

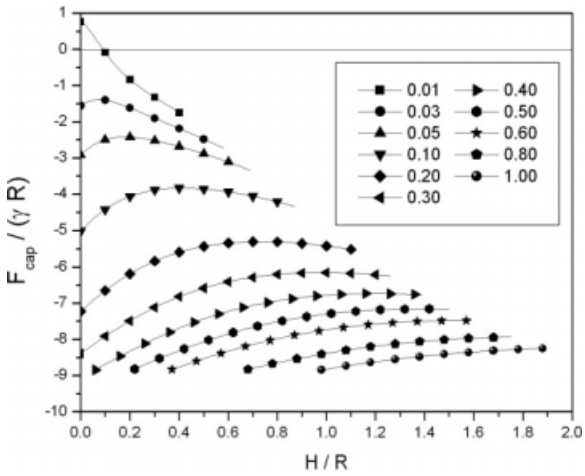

Figure 5. Dimensionless capillary force, F_{cap}, scaled by the product γR, Eq. 14, as a function of the dimensionless separation between particles, for the relative liquid volumes indicated in the legend, at $\theta = 20^\circ$.

$$\frac{F_{cap}}{\gamma R} = -2\pi \sin\alpha \sin(\alpha + \theta) - \pi R \sin^2\alpha \left(\frac{1}{L} - \frac{1}{\rho}\right) \quad (14)$$

where the first term corresponds to the wetting force and the second to the Laplace force, and γ is the surface tension of the liquid.

For a certain value of interparticle distance, H, relative volume of liquid respect to the solid, V_{rel}, and wetting angle, θ, the dimensionless capillary force, Eq. 14, may be obtained at these conditions. Figure 5 displays some results when the wetting angle is $\theta = 20^\circ$, at different liquid volumes and distances between the solid particles. Notice the truncation of the plots according to the corresponding H_{min} and H_{break}, for each liquid volume, V_{rel}, discussed earlier.

In general terms, it is observed that the capillary force shows two characters, repulsive and attractive, arising mainly from the behavior of the Laplace component. As the principal radii ρ and L have opposite signs this component may feature both characters. Repulsive Laplace forces are only observed in a small section of Region I, Figure 4, for liquid volumes, V_{rel}, smaller than 0.1 and wetting angles below 79.2°, conditions where the liquid meniscus is highly curved. For small distances and small liquid amounts, the Laplacian repulsion is able to dominate over the always attractive wetting force. This behavior is quite limited and beyond a certain distance between the solid surfaces, the capillary force becomes attractive. This is also the case when the liquid volume is larger; then, the total force is attractive in any combination $V_{rel} - \theta$ where it exists, Figure 4. Under this circumstance, the attractive capillary force increases its magnitude for increasing volumes of liquid due to an increase in contact area between the liquid and solid.

The maxima (minima in attraction) showed by F_{cap} obeys to the behavior of the Laplace component, which also shows a maximum. The maxima displayed in Figure 5 is found at

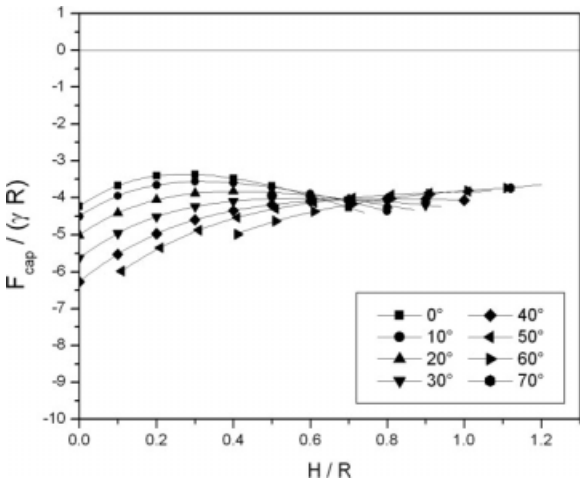

Figure 6. Dimensionless capillary force, $F_{cap}/(\gamma R)$, as a function of the separation between particles made dimensionless by the particles radius, R, for the wetting angles indicated, when $V_{rel} = 0.1$.

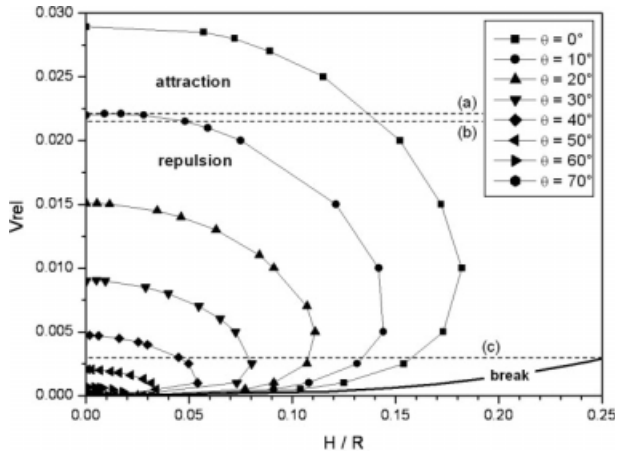

Figure 8. Values of the relative volume of liquid, V_{rel}, as a function of the dimensionless distances, H/R, for which $F_{cap} = 0$, at different wetting angles, θ.

The dotted lines separate the different patterns of the behavior of the system. The solid line indicates the bridge's break.

larger distances with increasing V_{rel}, this behavior also reported in literature.[6,29] For the largest liquid volumes the maximum is not observed because the liquid bridge is earlier destroyed at such long distances.

Figure 6 shows results of the dimensionless $F_{cap}/(\gamma R)$ for a fixed liquid volume, $V_{rel} = 0.1$, at different wetting angles, θ, at increasing separation distances, H/R, inside the ranges of existence. In agreement with the map displayed in Figure 4, there are values of the capillary force, always attractive at these conditions, for wetting angles up to $\approx 70°$. The force shows at each θ a maximum, representing a minimum in attraction, which overall result is that the different curves cross at $\approx 0.7R$. Before this cross over point, F_{cap} increases when increasing the angle, for later reverse this behavior. Notice that for the largest angles, the liquid bridge is found only in a very restricted range of interparticle distances, Figure 6, in agreement with the diagram displayed in Figure 4.

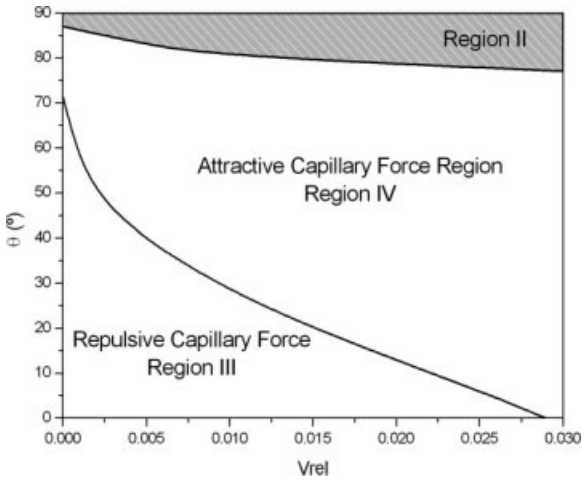

Figure 7. Map, $\theta - V_{rel}$, displaying the regions of repulsive (Region III) and attractive (Region IV) capillary forces, both inside Region I.

The Region II is shadowed for denoting its exclusion character.

As we have detected the possibility of repulsive capillary forces, already noticed in literature in both theoretical[25,30] and experimental approaches,[5] we proceed to outline the conditions for which the capillary force is repulsive. An exhaustive analysis of the capillary force as a function of the variables H, V_{rel}, and θ, enables us to delimit the regions of repulsive and attractive capillary forces, Figure 7. The capillary force is repulsive just for relative liquid volumes, V_{rel}, smaller than 0.03, and wetting angles, θ, below 71.6° (Region III). In the rest of Region I, Figure 4, the capillary force is always attractive (Region IV).

Considering the dimensionless distances, H/R, at which $F_{cap} = 0$, it is possible to distinguish several patterns of a system conformed by concave liquid bridges. Figure 8 shows these distances for different wetting angles, θ. Let us to consider, i.e., the particular case $\theta = 10°$, considering that its discussion is valid for the rest of cases, all similar in qualitative terms. Above line (a), there is attraction at any distance. Between lines (a) and (b) three situations may happen: attraction at very short distances, repulsion at intermediates and attraction again for larger H. This means that, if for any reason, the particles may move respect to each other, the whole system will shrink; then it will swell and finally, shrink again. The zone between lines (b) and (c) corresponds to swelling at moderate distances and shrinkage at larger ones, limited by the bridge break-up, line (c), below that the formation of a liquid bridge is not possible.

This behavior may have an impact in industrial processes like the storage and pipe transport of powders or granular matter like flours, cements, etc. An undesired absorption of very small amounts of water from ambient moisture may develop repulsive forces between the particles, and because of

them, the material can swell enough for obstructing the conductions and avoid completely its delivery from the silos or its transport throughout the pipes.

Conclusions

In the present work, we have mapped the region (in terms of the relative liquid volume, V_{rel}, and wetting angle, θ) of possible existence of a concave liquid bridge, indicating the particle separation for which the liquid bridge may be found. With this map, one can predict a priori, if a particular set of experimental conditions will be able to follow in a stable liquid bridge or not, and in positive case, at which particle separations.

Inside the region of existence, we have determined those regions where the capillary force is repulsive, zero and attractive. With this mapping effort, the experimental behavior of a real system may be predicted by just locating those particular experimental conditions in the maps. This is of great advantage when dealing with the stability and general behavior of a multiphase system where such liquid bridges are present.

Summarizing, our results indicate that stable liquid bridges cannot be formed for liquid volumes larger that 2 times the sphere's volume, independently of the value of the wetting angle. The Laplace component of the force may be attractive and repulsive, even if the meniscus keeps the concave shape, and this character is transmitted to the capillary force, and therefore, the later is found to be also repulsive for relative liquid volume lower than 0.03. For the rest of possible liquid volumes, the capillary force is found to be attractive.

Literature Cited

1. Dealy RB, Cahn JW. An analysis of the capillary forces in liquid-phase sintering of spherical particles. *Met Trans*. 1970;1:185–189.
2. Gonzenbach UT, Studart AR, Tervoort E, Gauckler LJ. Stabilization of foams with inorganic colloidal particles. *Langmuir*. 2006;22:10983–10988.
3. Haines WB. Studies in the physical properties of soils. *J Agric Sci*. 1925;15:529–543.
4. Fischer RA. On the capillary forces in an ideal soil: correction of the formulae given by W.B. Haines. *J Agric Sci*. 1926;16:492–505.
5. Huppmann WJ, Rieger H. Modelling of rearrangement processes in liquid phase sintering. *Acta Met*. 1975;23:965–971.
6. Pietsch W, Rumpf H. Haftkraft, Kapillardrudr, Fliissigkeitsvolumen und Grenzwinkel einer Fliissigkeitsbriicke zwischen zwei Kugeln. *Chemie Ing Tech*. 1967;39:885–893.
7. Chan DYC, Henry JD, White LR. The interaction of colloidal particles collected at fluid interfaces. *J Colloid Interface Sci*. 1981;79:410–418.
8. Erle MA, Dyson DC, Morrow NR. Liquid bridges between cylinders, in a torus, and between spheres. *AIChE J*. 1971;17:115–121.
9. Hotta K, Takeda K, Iinoya K. Capillary binding force of a liquid bridge. *Powder Technol*. 1974;10:231–242.
10. Orr FM, Scriven LE, Rivas AP. Pendular rings between solids—meniscus properties and capillary force. *J Fluid Mech*. 1975;67:723–742.
11. Mehrotra VP, Sastry KVS. Pendular bond strength between unequal-sized spherical-particles. *Powder Technol*. 1980;25:203–214.
12. De Bisschop FRE, Rigole WJL. A physical model for liquid capillary bridges between adsorptive solid spheres—the nodoid of Plateau. *J Colloid Interface Sci*. 1982;88:117–128.
13. Bayramli E, Abou-Obeid A, van de Ven TGM. Liquid bridges between spheres in a gravitational field. *J Colloid Interface Sci*. 1987;116:490–502.
14. Eremenko VN, Naidich YV, Lavrinenko IA. *Liquid-Phase Sintering*. New York: Consultants Bureau, 1970.
15. Meurisse MH, Querry M. Squeeze effects in a flat liquid bridge between parallel solid surfaces. *J Tribol*. 2006;128:575–584.
16. Mazzone DN, Tardos GI, Pfeffer R. The effect of gravity on the shape and strength of a liquid bridge between 2 spheres. *J Colloid Interface Sci*. 1986;113:544–556.
17. Dai ZF, Lu SC. Liquid bridge rupture distance criterion between spheres. *Int J Miner Proc*. 1998;53:171–181.
18. Delaunay DE. Sur la surface de revolution dont la courbure moyenne est constante. *J Math Pure Appl*. 1841;6:309–320.
19. Delannay F. Modelling of the influence of dihedral angle, volume fractions, particle size and coordination on the driving forces for sintering of dual phase systems. *Philos Mag*. 2005;85:3719–3733.
20. Pugh RJ. Foaming, foam films, antifoaming and defoaming. *Adv Colloid Interface Sci*. 1996;64:67–142.
21. Liu J, Cardamone AL, German RM. Estimation of capillary pressure in liquid phase sintering. *Powder Met*. 2001;44:317–324.
22. Ravinovich YI, Esayanur MS, Moudgil BM. Capillary forces between two spheres with a fixed volume liquid bridge: theory and experiment. *Langmuir*. 2005;21:10992–10997.
23. Fairbrother RJ, Simons SJR. The rupture energy of liquid bridges between spheres; the effect of contact angle and separation distance on liquid bridges geometries. In: Proceedings of the World Congress on Particle Technology 3. Brighton, UK, 1998:110.
24. Denkov ND, Ivanov IB, Kralchevsky PA, Wasan DT. A Possible Mechanism of Stabilization of Emulsions by Solid Particles. *J Colloid Interface Sci*. 1992;150:589–593.
25. Lian GP, Thornton C, Adams MJ. A theoretical study of the liquid bridge forces between two rigid spherical bodies. *J Colloid Interface Sci*. 1993;161:138–147.
26. Kohonen MM, Geromichalos D, Scheel M, Schier C, Herminghaus S. On capillary bridges in wet granular materials. *Physica A*. 2004;339:7–15.
27. Willett CD, Adams MJ, Johnson SA, Seville JPK. Capillary bridges between two spherical bodies. *Langmuir*. 2000;16:9396–9405.
28. Chen JC, Sheu JC, Lee YT. Maximum stable length of nonisothermal liquid bridges. *Phys Fluids A*. 1990;2:1118–1123.
29. Tselishchev YG, Val'tsifer VA. Influence of the type of contact between particles joined by a liquid bridge on the capillary cohesive forces. *Colloid J*. 2003;65:385–389.
30. Anestiev LA, Froyen LJ. Model of the primary rearrangement processes at liquid phase sintering and selective laser sintering due to biparticle interactions. *Appl Phys*. 1999;86:4008–4017.

Manuscript received Apr. 18, 2008, revision received Aug. 18, 2008, and final revision received Oct. 6, 2008.